Delivery Guarantee of Greedy Routing in Three Dimensional Wireless Networks

Yu Wang[1,⋆], Chih-Wei Yi[2,⋆⋆], and Fan Li[3]

[1] University of North Carolina at Charlotte, USA
yu.wang@uncc.edu
[2] National Chiao Tung University, Taiwan
yi@cs.nctu.edu.tw
[3] Beijing Institute of Technology, China
fli@bit.edu.cn

Abstract. In this paper, we investigate how to design greedy routing to guarantee packet delivery in a three-dimensional (3D) network. In 2D networks, many position-based routing protocols apply face routing on planar routing structure as a backup method to guarantee packet delivery when greedy routing fails at local minimum. However, in 3D networks, no planar topology can be constructed anymore. Even worse, a recent result [6] showed that there is no deterministic localized routing algorithm that guarantees the delivery of packets in 3D networks. Therefore, we propose to set up the transmission radius large enough to eliminate local minimum in the 3D network. In particular, we study the asymptotic critical transmission radius for greedy routing to ensure the packet delivery in randomly deployed 3D networks. Using similar techniques in [12], we theoretically prove that for a 3D network, formed by nodes that are produced by a Poisson point process of density n over a convex compact region of unit volume, $\sqrt[3]{\frac{3\beta_0 \ln n}{4\pi n}}$ is asymptotically almost surely (abbreviated by a.a.s.) the threshold of the critical transmission radius for 3D greedy routing, where $\beta_0 = 3.2$. We also conduct extensive simulations to confirm our theoretical results.

1 Introduction

Most existing wireless systems and protocols are based on two-dimensional (2D) design, where all wireless nodes are distributed in a two dimensional plane. This assumption is somewhat justified for applications where wireless devices are deployed on earth surface and where the height of the network is smaller than transmission radius of a node. However, 2D assumption may no longer be valid if a wireless network is deployed in space, atmosphere, or ocean, where nodes of a network are distributed over a 3D space and the difference in the third dimension is too large to be ignored. In fact, recent interest in ad hoc and sensor networks (such as underwater sensor networks [2])

⋆ This work of Yu Wang is supported in part by the US National Science Foundation (NSF) under Grant No. CNS-0721666.

⋆⋆ This work of Chih-Wei Yi is supported in part by the NSC under Grant No. NSC95-2221-E-009-059-MY3, by the ITRI under Grant No. 7301XS2220, and by the MoE ATU plan.

Y. Li et al. (Eds.): WASA 2008, LNCS 5258, pp. 4–16, 2008.

hints at the strong need to design 3D wireless networks. Most current research in 3D networks [11,3,13] primarily focuses on coverage and connectivity issues. In this paper, we study 3D localized position-based routing.

Localized position-based routing makes the forwarding decision based solely on the position information of the destination and local neighbors. It does not need the dissemination of route discovery information and the maintenance of routing tables. Thus, it enjoys the advantages of lower overhead and higher scalability than other traditional routing protocols. The popular localized routing is *greedy routing*, where a node finds the next relay node whose distance to the destination is the smallest among all neighbors. It is easy to construct an example to show that greedy routing will not succeed to reach the destination but fall into a local minimum (a node without any "better" neighbors). There are two ways to guarantee the packet delivery for greedy routing in 2D networks: (1) applying face routing, or (2) using large enough transmission power. Many position-based routing protocols [5,8,9] applied face routing as a backup method to get out of the local minimum after simple greedy heuristic fails. The idea of face routing is to walk along the faces which are intersected by the line segment st between the source s and the destination t. To guarantee the packet delivery, face routing requires the underlying routing topology to be a planar graph (*i.e.*, no link/edge intersection). The other way to guarantee packet delivery is letting all nodes have sufficiently large transmission radii to avoid the existence of local minimum. Recently, Wan *et al.* [12] studied the *critical transmission radius* (CTR) of greedy routing to guarantee the packet delivery in randomly deployed 2D networks.

Though some protocols for 2D networks can be directly extended to 3D networks, the design of 3D networks is surprisingly more difficult than that of 2D. In case of position-based routing, the simple greedy routing can be easily extended to 3D. Several 3D routing protocols [10, 14] specifically designed for underwater sensor networks are just variations of simple greedy routing. However, to guarantee the packet delivery of 3D greedy routing is not straightforward and very challenging. In 3D networks, there is no planar topology concept any more, thus, face routing can not be applied directly to help the greedy routing getting out of local minimum. Fevens *et al.* [7, 1] proposed several 3D position-based routing protocols and tried to find a way to still use face routing to get out of the local minimum. Their basic idea is projecting the 3D network to a 2D plane (or multiple 2D planes), then applying the face routing in the plane. However, as shown in Figure 1 [7], a planar graph cannot be extracted from the projected graph. It is clear that removing either $v_3'v_4'$ or $v_1'v_2'$ will break the connectivity. In fact, Durocher *et al.* [6] have recently proven that *there is no deterministic localized routing algorithm for 3D networks that guarantees the delivery of packets.*

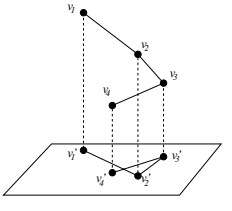

Fig. 1. A projection causes intersections

Therefore, in this paper, we adopt the second way to achieve delivery guarantee and provide a completed theoretical study on the critical transmission radius of 3D greedy routing that guarantees the delivery of packets between any source-destination pairs. We prove that for a 3D network, formed by nodes that are generated by a Poisson

point process of density n over a convex compact region of unit volume, the critical transmission radius for 3D greedy routing is a.a.s. at most $\sqrt[3]{\frac{3\beta \ln n}{4\pi n}}$ for any $\beta > \beta_0$ and at least $\sqrt[3]{\frac{3\beta \ln n}{4\pi n}}$ for any $\beta < \beta_0$. Here, $\beta_0 = 3.2$.

2 Preliminaries

2.1 Critical Transmission Radius for Greedy Routing

In any greedy-based routing, the packet may be dropped by some intermediate node u before it reaches the destination t when node u could not find any of its neighbors that is "better" than itself. One way to ensure that the routing is successful for every source-destination pairs is during the topology control (or power control) phase each wireless node is set with a sufficiently large transmission radius such that each intermediate node u will always find a better neighbor. Critical transmission radius for routing algorithm is first studied by [12]. Here, we review its definition as in [12]. Assume that V is the set of all wireless nodes in the network and each wireless node has a transmission radius r. Let $B(x, r)$ denote the open disk of radius r centered at x. Let

$$\rho(V) = \max_{\substack{(u,v)\in V^2 \\ u\neq v}} \min_{w\in B(v,\|u-v\|)} \|w-u\|.$$

In the equation, (u, v) is a source-destination pair. Since $w \in B(v, \|u - v\|)$, we have $\|w - v\| < \|u - v\|$. It means w is closer to v than u. If the transmission radius is not less than $\|w - u\|$, w might be the one to relay packets from u to v. Therefore, for each (u, v), the minimum of $\|w - u\|$ over all nodes on $B(v, \|u - v\|)$ is the transmission radius that ensures there is at least one node that can relay packets from u to v, and the maximum of the minimum over all (u, v) pairs guarantees the existence of relay nodes between any source-destination pair. Clearly, if the transmission radius is at least $\rho(V)$, packets can be delivered between any source-destination pairs. On the other hand, if the transmission radius is less than $\rho(V)$, there must exist some source-destination pair, *e.g.*, the (u, v) that yields the value $\rho(V)$, such that packets can't be delivered. Therefore, $\rho(V)$ is called the *critical transmission radius* (CTR) for greedy routing that guarantees the delivery of packets between any source-destination pair of nodes among V. By assuming the nodes are randomly deployed in a unit area region, Wan *et al.* [12] proved that $\sqrt{\frac{\beta_1 \ln n}{\pi n}}$ is asymptotically almost surely the threshold of $\rho(V)$ for greedy routing in 2D networks, where $\beta_1 = 1/(\frac{2}{3} - \frac{\sqrt{3}}{2\pi})$.

2.2 Assumptions and Notations

In this paper, we consider the deliverability by the asymptotics of $\rho(V)$, where V is given by a Poisson point process. By proper scaling, we assume the wireless devices are represented by a Poisson point process of density n over a unit-volume cube $\mathbb{D}$. $Po(n)$ denotes a Poisson RV with mean n, and $\mathcal{P}_n(A)$ represents a Poisson point process of density n over a region A. Especially, $\mathcal{P}_n$ is shorthand for $\mathcal{P}_n(\mathbb{D})$. In what

follows, $\|x\|$ is the Euclidean norm of a point $x \in \mathbb{R}^3$ and $\|x-y\|$ is the Euclidean distance between two points $x, y \in \mathbb{R}^3$. For a countable and finite set S, we use $\#(S)$ to denote its cardinality. $|A|$ is shorthand for the volume of a measurable set $A \subset \mathbb{R}^3$. All integrals considered will be Lebesgue integrals. For a set $A \subset \mathbb{R}^3$, $diam(A)$ denotes the diameter of A, and ∂A denotes the topological boundary of A. Let $B(x,r)$ denote the open sphere of radius r centered at x. For any two points $u, v \in \mathbb{R}^3$, the intersection of two spheres of radii $\|u-v\|$ centered respectively at u and v, denoted by L_{uv}, is called the *biconvex* of u and v, i.e. $L_{uv} = B(u, \|u-v\|) \cap B(v, \|u-v\|)$, and $\|u-v\|$ is called the depth of the biconvex. An event is said to be *asymptotic almost sure* (a.a.s.) if it occurs with a probability converges to one as $n \to \infty$. To avoid trivialities, we tacitly assume n to be sufficiently large if necessary.

2.3 Geometric Preliminaries

We first provide several geometric lemmas which will be used in the proof of our result in next section. However, due to the space limit, we ignore the detailed proofs of them.

If $\|u-v\| = 1$, a straightforward calculation yields that $|L_{uv}| = \frac{5\pi}{12}$. The volume of a biconvex with respect to two unit-volume balls is $\frac{5\pi/12}{4\pi/3} = \frac{5}{16}$. Let $\beta_0 = \frac{16}{5} = 3.2$. Then, the volume of a biconvex with depth r is $\frac{1}{\beta_0}\left(\frac{4}{3}\pi r^3\right)$. The following lemma gives a lower bound of the volume of two intersecting biconvexes.

Lemma 1. *Assume $R > 0$ and $a_1, b_1, a_2, b_2 \in \mathbb{R}^3$. Let $z_1 = \frac{1}{2}(a_1+b_1)$, $r_1 = \|a_1-b_1\|$, $z_2 = \frac{1}{2}(a_2+b_2)$, and $r_2 = \|a_2-b_2\|$. If $r_1, r_2 \in \left[\frac{1}{2}R, R\right]$, $\|z_1-z_2\| \leq \sqrt{3}R$, $a_1, b_1 \notin L_{a_2b_2}$, and $a_2, b_2 \notin L_{a_1b_1}$, there exist a constant c such that*

$$|L_{a_1b_1} \cup L_{a_2b_2}| - |L_{a_1b_1}| \geq cR^2 \|z_1 - z_2\|.$$

For any convex compact set $C \subset \mathbb{R}^3$, C_{-r} denotes the set of points in C that are away from ∂C by at least r. Next lemma gives a lower bound of the volume of C_{-r}.

Lemma 2. *Given a convex compact set $C \subset \mathbb{R}^3$ with diameter at most d, $|C_{-r}| \geq |C| - \pi d^2 r$.*

An ε-tessellation is a technique that divides the 3D space by vertical planes perpendicular to either x-axis or y-axis and horizontal planes perpendicular to z-axis into equal-size cubes, called cells, in which cells are with width ε. Without loss of generality, we assume the origin is a corner of cells. In a tessellation, a polycube is a collection of cells intersecting with a convex compact set. The x-span (and y-span, z-span, respectively) of a polycube is the distance measured in the number of cells in the x-direction (and y-direction, z-direction, respectively). If the span of a convex compact set is s and the width of cells is l, the span of the corresponding polycube is at most $\lceil s/l \rceil + 1$.

Lemma 3. *If a convex compact set S consists of m cubes and τ is a positive integer constant, the number of polycubes with span at most τ and intersecting with S is $\Theta(m)$.*

Next, we introduce a technique to obtain the Jacobian determinant in the change of variables that will be implicitly used in Subsection 3.2. Assume a tree topology is fixed

over $x_1, x_2, \cdots, x_k \in \mathbb{R}^3$. Without loss of generality, we may assume (x_{k-1}, x_k) is one of edges. Let $z_{k-1} = \frac{1}{2}(x_{k-1} + x_k)$ and (r, ϕ, θ) be the spherical coordinate of x_k with the origin at z_{k-1}. In other words, $(x_k - z_{k-1})_X = r\sin\phi\cos\theta$, $(x_k - z_{k-1})_Y = r\sin\phi\sin\theta$, and $(x_k - z_{k-1})_Z = r\cos\phi$. For $1 \le i \le k-2$, we use $p(x_i)$ to denote x_i's parent in the tree rooted at x_k, and let $z_i = \frac{1}{2}(x_i + p(x_i))$. Let $\mathbf{I}_3$ and $\mathbf{0}_3$ denote a 3×3 identity matrix and a 3×3 zero matrix respectively, and $\mathbf{J} = \begin{bmatrix} \sin\phi\cos\theta & r\cos\phi\cos\theta & -r\sin\phi\sin\theta \\ \sin\phi\sin\theta & r\cos\phi\sin\theta & r\sin\phi\cos\theta \\ \cos\phi & -\sin\phi & 0 \end{bmatrix}$ be the Jacobian matrix corresponding to changing variables from the Cartesian coordinate to the spherical coordinate. Then, the Jacobian determinant for changing variables $x_1, \cdots, x_{k-1}, x_k$ by $z_1, \cdots, z_{k-1}, (r, \phi, \theta)$ is $\left|\frac{\partial(x_1, \cdots, x_{k-1}, x_k)}{\partial(z_1, \cdots, z_{k-1}, r, \phi, \theta)}\right| = \left|\frac{\partial(x_1 + p(x_1), \cdots, x_{k-1} + p(x_{k-1}), x_k)}{\partial(z_1, \cdots, z_{k-1}, r, \phi, \theta)}\right| = 8^{k-1}\left|\frac{\partial\left(\frac{x_1 + p(x_1)}{2}, \cdots, \frac{x_{k-1} + p(x_{k-1})}{2}, x_k\right)}{\partial(z_1, \cdots, z_{k-1}, r, \phi, \theta)}\right|$

$= 8^{k-1}\left|\frac{\partial\left(\frac{x_1 + p(x_1)}{2}, \cdots, \frac{x_{k-1} + p(x_{k-1})}{2}, x_k\right)}{\partial(z_1, \cdots, z_{k-1}, r, \phi, \theta)}\right|$

$= 8^{k-1}\left|\frac{\partial(z_1, \cdots, z_{k-1}, x_k - z_{k-1})}{\partial(z_1, \cdots, z_{k-1}, r, \phi, \theta)}\right| = 8^{k-1}\begin{vmatrix} \mathbf{I}_3 & \cdots & \mathbf{0}_3 & \mathbf{0}_3 \\ \vdots & \ddots & \vdots & \vdots \\ \mathbf{0}_3 & \cdots & \mathbf{I}_3 & \mathbf{0}_3 \\ \mathbf{0}_3 & \cdots & \mathbf{0}_3 & \mathbf{J} \end{vmatrix} = 8^{k-1} r^2 \sin\phi$. In the first equality, each non-root variable is added by its parent variable. The equality stands since the Jacobian determinant is equal to 1 as we add one variable to another. Note that $\int_0^\pi \sin\phi d\phi = 2$.

2.4 Probabilistic Preliminaries

Let ϕ be the function over $(0, \infty)$ defined by $\phi(\mu) = 1 - \mu + \mu\ln\mu$. A straightforward calculation yields $\phi'(\mu) = \ln\mu$ and $\phi''(\mu) = 1/\mu$. Thus, ϕ is strictly convex and has the unique minimum zero at $\mu = 1$. Let $\phi^{-1} : [0, 1) \to (0, 1]$ be the inverse of the restriction of ϕ to $(0, 1]$. We define a function $\mathcal{L}$ over $(0, \infty)$ by

$$\mathcal{L}(\beta) = \begin{cases} \beta\phi^{-1}(1/\beta) & \text{if } \beta > 1, \\ 0 & \text{otherwise.} \end{cases}$$

It can be verified that $\mathcal{L}$ is a monotonic increasing function of β. The following lemma from [12] gives an estimation of the lower-tail distribution of Poisson RV's.

Lemma 4. *For any* $\mu \in (0, 1)$, $\lim_{\lambda\to\infty} \Pr(Po(\lambda) \le \mu\lambda) = \frac{1}{\sqrt{2\pi}} \frac{1}{\sqrt{\mu(1-\mu)}} \frac{1}{\sqrt{\lambda}} e^{-\lambda\phi(\mu)}$.

The next lemma gives a lower bound for the minimum of a collection of Poisson RVs. Due to space limit, we ignore its detailed proof.

Lemma 5. *Assume that* $\lim_{n\to\infty} \frac{\lambda_n}{\ln n} = \beta$ *for some* $\beta > 1$. *Let* $Y_1, Y_2, \cdots, Y_{I_n}$ *be* I_n *Poisson RVs with means at least* λ_n. *If* $I_n = o\left(n^s\sqrt{\ln n}\right)$ *for some real number* $s \in (0, 1]$, *then for any* $1 < \beta' < \beta$, $\min_{i=1}^{I_n} Y_i > s\mathcal{L}\left(\frac{1}{s}\beta'\right)\ln n$ *a.a.s.*.

At last, we state the Palm theory [4] on the Poisson process.

Theorem 1 ([4]). *Let $n > 0$. Suppose $k \in N$, and $h(\mathcal{Y}, \mathcal{X})$ is a bounded measurable function defined on all pairs of the form $(\mathcal{Y}, \mathcal{X})$ with $\mathcal{X} \subset \mathbb{R}^3$ being a finite subset and $\mathcal{Y}$ being a subset of $\mathcal{X}$, satisfying $h(\mathcal{Y}, \mathcal{X}) = 0$ except when $\mathcal{Y}$ has k elements. Then*

$$\mathbf{E}\left[\sum_{\mathcal{Y}\subseteq\mathcal{P}_n} h(\mathcal{Y}, \mathcal{P}_n)\right] = \frac{n^k}{k!}\mathbf{E}\left[h(\mathcal{X}_k, \mathcal{X}_k \cup \mathcal{P}_n)\right]$$

where the sum on the left side is over all subsets $\mathcal{Y}$ of the random Poisson point set $\mathcal{P}_n$, and on the right side the set $\mathcal{X}_k$ is a binomial process with k nodes, independent of $\mathcal{P}_n$.

We need to estimate the number of subsets with some specified topology, for example, two nodes are local minima w.r.t. each other. But it is not so easy to estimate this among Poisson point processes. The Palm theory allows us to place a set of random points first and then estimate the expectation over the Poisson point process. This technique will be used in Subsection 3.2 to prove Theorem 2(2).

3 Main Result: Critical Transmission Radius for 3D Greedy

The main result of our paper is the following theorem whose proof will be given in next two subsections.

Theorem 2. *Let $\beta_0 = 3.2$ and $n\left(\frac{4}{3}\pi r_n^3\right) = (\beta + o(1))\ln n$ for some $\beta > 0$. Then,*

1. *If $\beta > \beta_0$, then $\rho(\mathcal{P}_n) \leq r_n$ is a.a.s..*
2. *If $\beta < \beta_0$, then $\rho(\mathcal{P}_n) > r_n$ is a.a.s..*

To simplify the argument, we ignore boundary effects by assuming that there are nodes outside $\mathbb{D}$ with the same distribution. So, if necessary, packets can be routed through those nodes outside $\mathbb{D}$.

3.1 Upper Bound of Theorem 2

The upper bound in Theorem 2 is going to be proved through a technique called minimal scan statistics. For a finite point set V and a real number $r > 0$, we define $S(V, r) = \min_{u,v\in\mathbb{D},\|u-v\|=r} \#(V \cap L_{uv})$. $S(V, r)$ is the minimal number of nodes of V that can be covered by a biconvex with depth r. We claim that the event $S(\mathcal{P}_n, r_n) > 0$ implies the event $\rho(\mathcal{P}_n) \leq r_n$. Assume to the contrary that $\rho(\mathcal{P}_n) > r_n$. Then there exist a pair of nodes u and v such that u is a local minimum w.r.t. to v. In other words, $\|u - v\| > r_n$ and no other nodes of $\mathcal{P}_n$ are in $B(u, r_n) \cap B(v, \|u - v\|)$. Let w be the intersection point of the segment uv and the sphere $\partial B(u, r_n)$. Since $L_{uw} \subset B(u, r_n) \cap B(v, \|u - v\|)$, this implies that L_{uw} contains no nodes of $\mathcal{P}_n$. Thus, $S(\mathcal{P}_n, r_n) = 0$, which is a contradiction. So, our claim is true.

To have the lower bound of minimal scan statistics, we apply the tessellation technique to discretize the scanning process. We tessellate the deployment region by properly choosing cell size such that: (1) each copy of the biconvex contains a polycube with volume at least $\eta\frac{\ln n}{n}$ for some $\eta > 1$, and (2) the number of polycubes is $O\left(\frac{n}{\ln n}\right)$. Then, the next lemma follows Lemma 5.

Lemma 6. *Suppose that* $n\left(\frac{4}{3}\pi r_n^3\right) = (\beta + o(1))\ln n$ *for some* $\beta > \beta_0$. *Then for any constant* $\beta_1 \in (\beta_0, \beta)$, *it is a.a.s. that* $S(\mathcal{P}_n, r_n) > \mathcal{L}\left(\frac{\beta_1}{\beta_0}\right)\ln n$.

PROOF. Let $d = \sqrt{3}r_n$ which is the largest distance between any two points in a biconvex. For a given β_1, choose a constant $\beta_2 \in (\beta_1, \beta)$, and let $\varepsilon = \frac{4}{27\beta_0}\left(1 - \frac{\beta_2}{\beta}\right)$. Consider an εd-tessellation. (Note that ε is chosen such that each copy of the biconvex contains a polycube with volume at least $\eta\frac{\ln n}{n}$ for some $\eta > 1$.) To prove this inequality, it is sufficient to show that any biconvex of two points in $\mathbb{D}$ that are separated by a distance of r_n contains a polycube with span at most $\frac{1}{\varepsilon}$ and volume at least $\frac{\beta_2}{\beta_0}\left(\frac{4}{3}\pi r_n^3\right)\frac{1}{\beta}$.

For a biconvex L, let P denote the polycube induced by $L_{-\sqrt{3}\varepsilon d}$. Then, $P \subseteq L$, and the span of P is at most $\left\lceil \frac{d - 2\sqrt{3}\varepsilon d}{\varepsilon d} \right\rceil + 1 < \frac{1}{\varepsilon}$. By Lemma 2 and the fact that $|L| = \frac{4}{3}\pi r_n^3 \frac{1}{\beta_0} = \frac{4}{9\sqrt{3}}\pi d^3 \frac{1}{\beta_0}$, we have $|P| \geq \left|L_{-\sqrt{3}\varepsilon d}\right| \geq |L| - \pi d^2\left(\sqrt{3}\varepsilon d\right) = |L| - \sqrt{3}\varepsilon\pi d^3 = |L| - \frac{27\beta_0}{4}\varepsilon|L| > |L|\left(1 - \frac{27\beta_0}{4}\varepsilon\right) = \frac{\beta_2}{\beta}|L| = \frac{\beta_2}{\beta_0}\left(\frac{4}{3}\pi r_n^3\right)\frac{1}{\beta}$. Let I_n denote the number of polycubes in $\mathbb{D}$ with span at most $\frac{1}{\varepsilon}$ and volume at least $\frac{\beta_2}{\beta_0}\left(\frac{4}{3}\pi r_n^3\right)\frac{1}{\beta} = \left(\frac{\beta_2}{\beta_0} + o(1)\right)\frac{\ln n}{n}$, and Y_i be the number of nodes on the i-th polycubes. Then Y_i is a Poisson RV with rate at least $\left(\frac{\beta_2}{\beta_0} + o(1)\right)\ln n$. Since the number of cells in $\mathbb{D}$ is $O\left(\left(\frac{1}{\varepsilon d}\right)^3\right) = O\left(\frac{n}{\ln n}\right)$, by Lemma 3, $I_n = O\left(\frac{n}{\ln n}\right)$. By Lemma 5, it is a.a.s. that $\frac{\min_{i=1}^{I_n} Y_i}{\ln n} \geq \mathcal{L}\left(\frac{\beta_2}{\beta_0}\right) > \mathcal{L}\left(\frac{\beta_1}{\beta_0}\right)$. Thus, $\mathcal{S}(\mathcal{P}_n, r_n) \geq \min_{i=1}^{I_n} Y_i$. □

3.2 Lower Bound of Theorem 2

Theorem 2(2) can be proved by showing that if $r_n = \sqrt[3]{\frac{3\beta\ln n}{4\pi n}}$ for any $\beta < \beta_0$, there a.a.s. exists local minima. The space is going to be tessellated into equal-size cube cells. For each cell, an event that implies the existence of local minima in the cell is introduced, and a lower bound for the probability of the event is derived. Since these events are identical and independent over cells, we can estimate a probability lower of existence of local minima. By showing the lower bound is a.a.s. equal to 1, we prove Theorem 2(2). The detail is given below.

Let β_1 and β_2 be two positive constants such that $\max\left(\frac{1}{8}\beta_0, \beta\right) < \beta_1 < \beta_2 < \beta_0$. In addition, let R_1 and R_2 be given by $n\left(\frac{4}{3}\pi R_1^3\right) = \beta_1 \ln n$ and $n\left(\frac{4}{3}\pi R_2^3\right) = \beta_2 \ln n$, respectively. Since $\frac{1}{8}\beta_0 < \beta_1 < \beta_2 < \beta_0$, we have $\frac{1}{2}R_2 \leq R_1 \leq R_2$. Divide $\mathbb{D}$ by $\left(4\sqrt[3]{\frac{\ln n}{n\pi}}\right)$-tessellation. Let I_n denote the number of cells fully contained in $\mathbb{D}$. Here we have $I_n = O\left(\frac{n}{\ln n}\right)$. For each cell fully contained in $\mathbb{D}$, we draw a ball of radius $\frac{1}{2}\sqrt[3]{\frac{\ln n}{n\pi}}$ at the center of the cell. For $1 \leq i \leq I_n$, let E_i be the event that there exists two nodes $X, Y \in \mathcal{P}_n$ such that their midpoint is in the i-th ball, their distance is between R_1 and R_2, and there is no other node in L_{XY}. For any two nodes u and v with $\|u - v\| > r_n$, if there are no other nodes in L_{uv}, u and v are local minima w.r.t. each other. So, E_i implies existence of local minimum, and

$$\Pr\left[\rho\left(\mathcal{P}_n\right) > r_n\right] \geq \Pr\left[\text{at least one } E_i \text{ occurs}\right].$$

Let o_i denote the center of the i-th ball, and u, v be two points such that $\frac{1}{2}(u+v)$ is in the i-th ball and $R_1 \leq \|u-v\| \leq R_2$. By triangle inequality, for any point $w \in L_{uv}$, we have $\|w-o_i\| \leq \left\|w-\frac{1}{2}(u+v)\right\| + \left\|o_i-\frac{1}{2}(u+v)\right\| < \frac{\sqrt{3}}{2}\sqrt[3]{\frac{3\beta_0 \ln n}{4n\pi}} + \frac{1}{2}\sqrt[3]{\frac{\ln n}{n\pi}} < 2\sqrt[3]{\frac{\ln n}{n\pi}}$. Since the width of cells is $4\sqrt[3]{\frac{\ln n}{n\pi}}$, u, v, and L_{uv} are contained in the i-th cube. Therefore, $E_1, \cdots, E_{I_i}$ are independent. In addition, $E_1, \cdots, E_{I_i}$ are identical. Then,

$$\Pr\left[\text{none of } E_i \text{ occurs}\right] = \left(1-\Pr\left[E_1\right]\right)^{I_n} \leq e^{-I_n \Pr(E_1)}.$$

If $I_n \Pr\left(E_1\right) \to \infty$, we may have $\Pr\left[\rho\left(\mathcal{P}_n\right) > r_n\right] \to 1$, and Theorem 2(2) follows. Next, we will prove that $I_n \Pr\left(E_1\right) \to \infty$.

First, we introduce several relevant events and derive their probabilities. Let A denote the disk with radius $\frac{1}{2}\sqrt[3]{\frac{\ln n}{n\pi}}$ at the center of the first cube. Assume V is a point set and $T \subset V$. Let $h_1(T, V)$ denote a function such that $h_1\left(T=\{x_1, x_2\}, V\right) = 1$ only if $\frac{1}{2}(x_1+x_2) \in A$, $R_1 \leq \|x_1-x_2\| \leq R_2$, and there is no other node of V in $L_{x_1x_2}$; otherwise, $h_1(T, V) = 0$. In addition, under Boolean addition, for any $\{x_1, x_2, x_3\} \subseteq V$, let $h_2\left(\{x_1, x_2, x_3\}, V\right) = h_1\left(\{x_1, x_2\}, V\right) \cdot h_1\left(\{x_1, x_3\}, V\right) + h_1\left(\{x_2, x_1\}, V\right) \cdot h_1\left(\{x_2, x_3\}, V\right) + h_1\left(\{x_3, x_1\}, V\right) \cdot h_1\left(\{x_3, x_2\}, V\right)$; for any $\{x_1, x_2, x_3, x_4\} \subseteq V$, let $h_3\left(\{x_1, x_2, x_3, x_4\}, V\right) = h_1\left(\{x_1, x_2\}, V\right) \cdot h_1\left(\{x_3, x_4\}, V\right) + h_1\left(\{x_1, x_3\}, V\right) \cdot h_1\left(\{x_2, x_4\}, V\right) + h_1\left(\{x_1, x_4\}, V\right) \cdot h_1\left(\{x_2, x_3\}, V\right)$.

E_1 is the event that there exists two nodes $X, Y \in \mathcal{P}_n$ such that $h_1\left(\{X, Y\}, \mathcal{P}_n\right) = 1$. In the remaining of this subsection, we use X_1', X_2', X_3' and X_4' to denote elements of $\mathcal{P}_n$. Let $F_1'\left(\{X_1', X_2'\}\right)$ be the event that $h_1\left(\{X_1', X_2'\}, \mathcal{P}_n\right) = 1$; $F_2'\left(\{X_1', X_2', X_3'\}\right)$ be the event that $h_2\left(\{X_1', X_2', X_3'\}, \mathcal{P}_n\right) = 1$ which is the indicator of the event and $F_3'\left(\{X_1', X_2', X_3', X_4'\}\right)$ be the event that $h_3\left(\{X_1', X_2', X_3', X_4'\}, \mathcal{P}_n\right) = 1$. Applying Boole's inequalities, we have

$$\begin{aligned}\Pr\left[E_1\right] \geq & \sum_{\{X_1', X_2'\} \subseteq \mathcal{P}_n} \Pr\left[F_1'\left(\{X_1', X_2'\}\right)\right] - \sum_{\{X_1', X_2', X_3'\} \subseteq \mathcal{P}_n} \Pr\left[F_2'\left(\{X_1', X_2', X_3'\}\right)\right] \\ & - \sum_{\{X_1', X_2', X_3', X_4'\} \subseteq \mathcal{P}_n} \Pr\left[F_3'\left(\{X_1', X_2', X_3', X_4'\}\right)\right]. \end{aligned} \tag{1}$$

For the sake of clarity, we use X_1, X_2, X_3 and X_4 to denote independent random points with uniform distribution over $\mathbb{D}$ and independent of $\mathcal{P}_n$. Let F_1 be the event that $h_1\left(\{X_1, X_2\}, \{X_1, X_2\} \cup \mathcal{P}_n\right) = 1$,$F_2$ be the event that $h_2(\{X_1, X_2, X_3\}, \{X_1, X_2, X_3\} \cup \mathcal{P}_n) = 1$, and F_3 be the event that $h_3(\{X_1, X_2, X_3, X_4\}, \{X_1, X_2, X_3, X_4\} \cup \mathcal{P}_n) = 1$. According to the Palm theory (Theorem 1), we have

$$\begin{aligned}\sum_{\{X_1', X_2'\} \subseteq \mathcal{P}_n} \Pr\left[F_1'\left(\{X_1', X_2'\}\right)\right] &= \mathbf{E}\left[\sum_{\{X_1', X_2'\} \subseteq \mathcal{P}_n} h_1\left(\{X_1', X_2'\}, \mathcal{P}_n\right)\right] \\ &= \frac{n^2}{2!}\mathbf{E}\left[h_1\left(\{X_1, X_2\}, \{X_1, X_2\} \cup \mathcal{P}_n\right)\right] = \frac{n^2}{2}\Pr\left[F_1\right]; \end{aligned} \tag{2}$$

$$\sum_{\{X_1',X_2',X_3'\}\subseteq\mathcal{P}_n}\Pr\left[F_2'\left(\{X_1',X_2',X_3'\}\right)\right]=\mathbf{E}\left[\sum_{\{X_1',X_2',X_3'\}\subseteq\mathcal{P}_n}h_2\left(\{X_1',X_2',X_3'\},\mathcal{P}_n\right)\right]$$
$$=\frac{n^3}{3!}\mathbf{E}\left[h_2\left(\{X_1,X_2,X_3\},\{X_1,X_2,X_3\}\cup\mathcal{P}_n\right)\right]=3\frac{n^3}{3!}\Pr\left[F_2\right]=\frac{n^3}{2}\Pr\left[F_2\right];\tag{3}$$

$$\sum_{\{X_1',X_2',X_3',X_4'\}\subseteq\mathcal{P}_n}\Pr\left[F_3'\left(\{X_1',X_2',X_3',X_4'\}\right)\right]=\mathbf{E}\left[\sum_{\{X_1',X_2',X_3',X_4'\}\subseteq\mathcal{P}_n}h_3\left(\{X_1',X_2',X_3',X_4'\},\mathcal{P}_n\right)\right]$$
$$=\frac{n^4}{4!}\mathbf{E}\left[h_3\left(\{X_1,X_2,X_3,X_4\},\{X_1,X_2,X_3,X_4\}\cup\mathcal{P}_n\right)\right]=3\frac{n^4}{4!}\Pr\left[F_3\right]=\frac{n^4}{8}\Pr\left[F_3\right].\tag{4}$$

From Eq. (1), (2), (3), and (4), we have

$$\Pr\left[E_1\right]\geq\frac{n^2}{2}\Pr\left[F_1\right]-\frac{n^3}{2}\Pr\left[F_2\right]-\frac{n^4}{8}\Pr\left[F_3\right].\tag{5}$$

In the next, we will derive the probabilities of F_1, F_2, and F_3. Let S_1 denote the set $\left\{(x_1,x_2)\,\middle|\,\frac{1}{2}(x_1+x_2)\in A,R_1\leq\|x_1-x_2\|\leq R_2\right\}$. We have

$$\begin{aligned}\Pr\left[F_1\right]&=\int\int_{S_1}\Pr\left[F_1\mid X_1=x_1,X_2=x_2\right]dx_1dx_2\\&=\int\int_{S_1}e^{-n\left|L_{x_1x_2}\right|}dx_1dx_2=\int\int_{S_1}e^{-n\frac{1}{\beta_0}\left(\frac{4}{3}\pi\left\|x_1-x_2\right\|^3\right)}dx_1dx_2.\end{aligned}$$

Let $z=\frac{x_1+x_2}{2}$ and $r=\frac{1}{2}\|x_1-x_2\|$. Then,

$$\begin{aligned}\Pr\left[F_1\right]&=\int_{z\in A}\int_{r=\frac{R_1}{2}}^{\frac{R_2}{2}}e^{-\frac{n}{\beta_0}\frac{32}{3}\pi r^3}32\pi r^2drdz=\int_{z\in A}\int_{r=\frac{R_1}{2}}^{\frac{R_2}{2}}e^{-\frac{n}{\beta_0}\frac{32}{3}\pi r^3}d\left(\frac{32}{3}\pi r^3\right)dz\\&=-\left(\frac{\beta_0}{n}e^{-\frac{n}{\beta_0}\frac{32}{3}\pi r^3}\Big|_{r=\frac{R_1}{2}}^{\frac{R_2}{2}}\right)|A|=\frac{\beta_0}{6n^2}\left(n^{-\frac{\beta_1}{\beta_0}}-n^{-\frac{\beta_2}{\beta_0}}\right)\ln n.\end{aligned}\tag{6}$$

Let S_2 denote the set $\left\{(x_1,x_2,x_3)\,\middle|\,\begin{array}{l}\frac{x_1+x_2}{2},\frac{x_1+x_3}{2}\in A;\\R_1\leq\|x_1-x_2\|\leq R_2;x_1,x_2\notin L_{x_1x_3};\\R_1\leq\|x_1-x_3\|\leq R_2;x_1,x_3\notin L_{x_1x_2}\end{array}\right\}$. Applying Lemma 1, if $(x_1,x_2,x_3)\in S_2$, we have

$$\begin{aligned}\Pr\left[F_2\right]&=\int\int\int_{S_2}\Pr\left[F_2\,\middle|\,\begin{array}{c}X_i=x_i\\\forall i=1,2,3\end{array}\right]dx_1dx_2dx_3\\&\leq3\int\int\int_{S_2}e^{-n\left|L_{x_1x_2}\cup L_{x_1x_3}\right|}dx_1dx_2dx_3\\&\leq3\int\int\int_{S_2}e^{-n\left(\frac{1}{\beta_0}\frac{4}{3}\pi\|x_1-x_2\|^3+cR_2^2\left\|\frac{x_1+x_2}{2}-\frac{x_1+x_3}{2}\right\|\right)}dx_1dx_2dx_3.\end{aligned}$$

Let $z_1 = \frac{x_1+x_2}{2}$, $z_2 = \frac{x_1+x_3}{2}$, $r = \frac{\|x_1-x_2\|}{2}$, and $\rho = \|z_1 - z_2\|$. Then,

$$\begin{aligned}
\Pr[F_2] &\le 3\int_{z_1\in A}\int_{r=\frac{R_1}{2}}^{\frac{R_2}{2}}\int_{z_2\in A} e^{-n\left(\frac{1}{\beta_0}\frac{32}{3}\pi r^3 + cR_2^2\|z_1-z_2\|\right)}\cdot 256\pi r^2 dr dz_1 dz_2 \\
&\le 24\int_{z_1\in A}\int_{r=\frac{R_1}{2}}^{\frac{R_2}{2}} e^{-\frac{n}{\beta_0}\left(\frac{32}{3}\pi r^3\right)} d\left(\frac{32}{3}\pi r^3\right) dz_1 \cdot \int_{z_2\in A} e^{-cnR_2^2\|z_1-z_2\|} dz_2 \\
&\le 24\int_{z_1\in A}\int_{r_1=\frac{R_1}{2}}^{\frac{R_2}{2}} e^{-\frac{n}{\beta_0}\left(\frac{32}{3}\pi r^3\right)} d\left(\frac{32}{3}\pi r^3\right) dz_1 \cdot \int_{\rho=0}^{\infty} e^{-cnR_2^2\rho} 4\pi\rho^2 d\rho \\
&= 24\left(\frac{\beta_0}{6n^2}\left(n^{-\frac{\beta_1}{\beta_0}} - n^{-\frac{\beta_2}{\beta_0}}\right)\ln n\right)\left(\frac{8\pi}{(cnR_2^2)^3}\right) \\
&= \frac{32\pi\beta_0}{c^3\left(nR_2^3\right)^2 n^3}\left(n^{-\frac{\beta_1}{\beta_0}} - n^{-\frac{\beta_2}{\beta_0}}\right)\ln n. \qquad (7)
\end{aligned}$$

Let S_3 denote the set $\left\{(x_1,x_2,x_3,x_4)\left|\begin{array}{c}\frac{x_1+x_2}{2}, \frac{x_3+x_4}{2}\in A; \\ R_1\le\|x_1-x_2\|\le R_2; x_1,x_2\notin L_{x_3x_4}; \\ R_1\le\|x_3-x_4\|\le R_2; x_3,x_4\notin L_{x_1x_2}\end{array}\right.\right\}$. Applying Lemma 1, if $(x_1,x_2,x_3,x_4)\in S_3$, we have

$$\begin{aligned}
\Pr[F_3] &= \int\int\int\int_{S_3}\Pr\left[F_3\left|\begin{array}{c}X_i = x_i, \\ \forall i = 1,2,3,4\end{array}\right.\right] dx_1dx_2dx_3dx_4 \\
&\le 3\int\int\int\int_{S_3} e^{-n\left|L_{x_1x_2}\cup L_{x_3x_4}\right|} dx_1dx_2dx_3dx_4 \\
&\le 3\int\int\int\int_{S_3} e^{-n\left(\frac{1}{\beta_0}\frac{4}{3}\pi\|x_1-x_2\|^3 + cR_2^2\left\|\frac{x_1+x_2}{2}-\frac{x_3+x_4}{2}\right\|\right)}\cdot dx_1dx_2dx_3dx_4.
\end{aligned}$$

Let $z_1 = \frac{x_1+x_2}{2}$, $r_1 = \frac{\|x_1-x_2\|}{2}$, $z_2 = \frac{x_3+x_4}{2}$, $r_2 = \frac{\|x_3-x_4\|}{2}$, and $\rho = \|z_1 - z_2\|$. Then,

$$\begin{aligned}
&\Pr[F_3] \le 3\int_{z_1\in A}\int_{r_1=\frac{R_1}{2}}^{\frac{R_2}{2}}\int_{z_2\in A}\int_{r_2=\frac{R_1}{2}}^{\frac{R_2}{2}} e^{-n\left(\frac{1}{\beta_0}\frac{32}{3}\pi r_1^3 + cR_2^2\|z_1-z_2\|\right)}\cdot\left(32\pi r_1^2 dr_1 dz_1\right)\left(32\pi r_2^2 dr_2 dz_2\right) \\
&\le 3\left(\int_{z_1\in A}\int_{r_1=\frac{R_1}{2}}^{\frac{R_2}{2}} e^{-\frac{n}{\beta_0}\frac{32}{3}\pi r_1^3} d\left(\frac{32}{3}\pi r^3\right) dz\right)\left(32\pi\left(\frac{R_2}{2}\right)^2\left(\frac{R_2}{2}-\frac{R_1}{2}\right)\int_{\rho=0}^{\infty} e^{-cnR_2^2\rho} 4\pi\rho^2 d\rho\right) \\
&= \frac{16\pi^2\beta_0}{c^3\left(nR_2^3\right)n^4}\left(1-\frac{R_1}{R_2}\right)\left(n^{-\frac{\beta_1}{\beta_0}} - n^{-\frac{\beta_2}{\beta_0}}\right)\ln n.
\end{aligned} \qquad (8)$$

Put Eq. (5), (6), (7) and (8) together. We have

$$\begin{aligned}
\Pr[E_1] &\ge \left(\frac{\beta_0}{12} - \frac{16\pi\beta_0}{c^3\left(nR_2^3\right)^2} - \frac{2\pi^2\beta_0}{c^3\left(nR_2^3\right)}\left(1-\frac{R_1}{R_2}\right)\right)\left(n^{-\frac{\beta_1}{\beta_0}} - n^{-\frac{\beta_2}{\beta_0}}\right)\ln n \\
&\sim \frac{\beta_0}{12}\left(n^{-\frac{\beta_1}{\beta_0}} - n^{-\frac{\beta_2}{\beta_0}}\right)\ln n.
\end{aligned}$$

Since $I_n = \Omega\left(\frac{\ln n}{n}\right)$, we have $\Pr[E_1] = \Omega\left(\left(n^{-\frac{\beta_1}{\beta_0}} - n^{-\frac{\beta_2}{\beta_0}}\right)\ln n\right)$, and $I_n\Pr[E_1] = \Omega\left(n^{1-\frac{\beta_1}{\beta_0}}\right)\to\infty$. This complete the proof of Theorem 2(2).

4 Simulation

We have analyzed the theoretical bounds of the critical transmission radius for 3D greedy routing. To confirm our theoretical analysis, we conduct several simulations to see what is the practical value of transmission radius (r) such that greedy can guarantee the packet delivery with high probability in random networks.

Critical Transmission Radius for Random Networks: We randomly generate 1000 networks with n wireless nodes in a $20 \times 20 \times 20$ cubic region, where n is from 100 to 500. For each network V, we compute the critical transmission radius $\rho(V)$ by definition (the equation in Section 2.1). Figure 2 gives the histograms of the distribution of $\rho(V)$ for 1000 random networks. Figure 4(a) shows the probability distribution function of $\rho(V)$. It is clear that the critical transmission radius satisfies a transition phenomena, i.e., there is a radius r_0 such that the greedy can successfully deliver the packet when $r > r_0$ and can not deliver the packet when $r < r_0$. We also find that the transition becomes faster when the number of nodes increases. Notice that the practical value of $\rho(V)$ is larger than the theoretical bound in our analysis. Remember the theoretical bound is true for $n \to \infty$. However, the practical value will approach the theoretical bound with the increasing of n . When $n = 500$, it already becomes very near the theoretical bound. When $n = 500$, the theoretical bound is $\sqrt[3]{\frac{3\beta_0 \ln n}{4\pi n}} \times 20 = 0.212 \times 20 = 4.24$ for a $20 \times 20 \times 20$ cubic region.

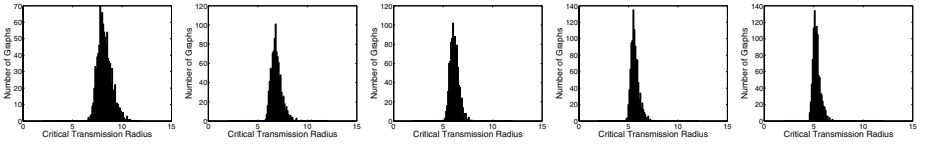

(a) 100 Nodes (b) 200 Nodes (c) 300 Nodes (d) 400 Nodes (e) 500 Nodes

Fig. 2. The distribution of $\rho(V)$ for random networks with 100-500 nodes

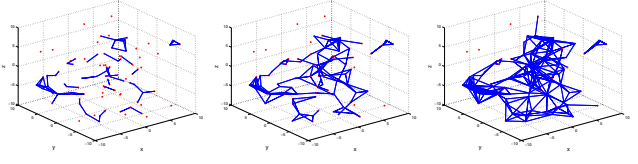

(a) $r = 3$ (b) $r = 4$ (c) $r = 5$

(d) $r = 6$ (e) $r = 7$ (f) $r = 8$

Fig. 3. Network topologies with 100 nodes when r is from 3 to 8

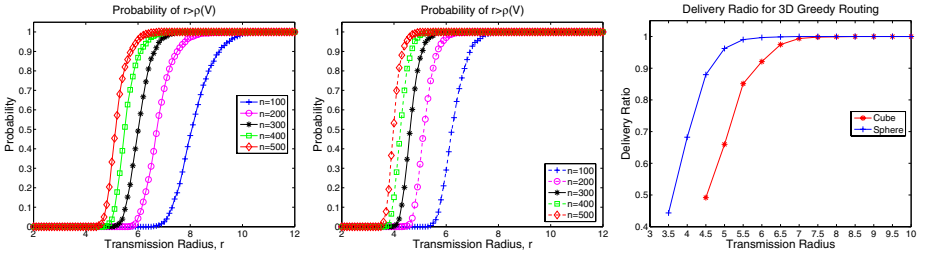

(a) PDF for $20 \times 20 \times 20$ cubic (b) PDF for sphere with radius 20 (C) Delivery Ratio

Fig. 4. (a) and (b): the probability distribution function of $\rho(V)$ for cubic and sphere networks; (c): delivery ratio for 100-node random networks with various r

Delivery Ratio of Greedy Routing with Various Transmission Radii. We implement the 3D greedy routing in our simulator. By setting various transmission radii, we generate 100 random networks with 100 wireless nodes again in a $20 \times 20 \times 20$ cubic region. Figure 3 shows a set of examples when the transmission radius r is from 3 to 8. Notice that when $r \leq 5$, the network is not connected. In this simulation, we only consider the connected networks. We randomly select 100 source-destination pairs for each connected network and test the 3D greedy routing. Figure 4(c) (the blue curve marked by crosses) illustrate the average delivery ratio of 3D greedy routing. Clearly, the delivery ratio increases when r increases. After r is larger than a certain value, it always guarantee the delivery. This also confirms our theoretical analysis. In addition, from Figure 3 and Figure 4(c), we can conclude that the CTR for greedy routing (approaching 100% delivery ratio when r is around 7 in Figure 4(c)) is just a little bit larger than the CTR for connectivity (network becomes connected when r is around 6 in Figure 3).

Besides deploying random networks in a cubic region, we also performed simulations for networks deployed in a spherical region (with 20 as its radius). Figure 4(b) gives the probability distribution function of $\rho(V)$ and Figure 4(c)(the red curve marked by stars) illustrates the average delivery ratio of 3D greedy routing. The conclusions from these simulations are consistent with the simulations for random network deployed in cubic region.

5 Conclusion

In this paper, we study the critical transmission radius for 3D greedy routing which leads to a delivery-guaranteed 3D localized routing. We theoretically prove that for a random 3D network, formed by nodes that are generated by a Poisson point process of density n over a convex compact region of unit volume, the critical transmission radius for 3D greedy routing is a.a.s. $\sqrt[3]{\frac{3\beta_0 \ln n}{4\pi n}}$, where $\beta_0 = 3.2$. This theoretical result answers a fundamental question about how large the transmission radius should be set in a 3D networks, such that the greedy routing guarantees the delivery of packets between any two nodes. We also conduct extensive simulations to confirm our theoretical results.

References

1. Abdallah, A., Fevens, T., Opatrny, J.: Power-aware 3D position-based routing algorithm for ad hoc networks. In: Proc. of IEEE ICC (2007)
2. Akyildiz, I.F., Pompili, D., Melodia, T.: Underwater acoustic sensor networks: research challenges. Ad Hoc Networks 3(3), 257–279 (2005)
3. Alam, S.M.N., Haas, Z.J.: Coverage and connectivity in three-dimensional networks. In: Proc. of ACM Mobicom (2006)
4. Baccelli, F., Bremaud, P.: Elements of Queueing Theory: Palm-Martingale Calculus and Stochastic Recurrences. Springer, Heidelberg (2003)
5. Bose, P., Morin, P., Stojmenovic, I., Urrutia, J.: Routing with guaranteed delivery in ad hoc wireless networks. ACM/Kluwer Wireless Networks 7(6) (2001)
6. Durocher, S., Kirkpatrick, D., Narayanan, L.: On routing with guaranteed delivery in three-dimensional ad hoc wireless networks. In: Rao, S., Chatterjee, M., Jayanti, P., Murthy, C.S.R., Saha, S.K. (eds.) ICDCN 2008. LNCS, vol. 4904, pp. 546–557. Springer, Heidelberg (2008)
7. Kao, G., Fevens, T., Opatrny, J.: Position-based routing on 3D geometric graphs in mobile ad hoc networks. In: Proc. of CCCG 2005 (2005)
8. Karp, B., Kung, H.: GPSR: Greedy perimeter stateless routing for wireless networks. In: Proc. of the ACM Int'l Conf. on Mobile Computing and Networking (2000)
9. Kuhn, F., Wattenhofer, R., Zollinger, A.: Worst-Case Optimal and Average-Case Efficient Geometric Ad-Hoc Routing. In: Proc. of ACM MobiHoc (2003)
10. Pompili, D., Melodia, T.: Three-dimensional routing in underwater acoustic sensor networks. In: Proceedings of ACM PE-WASUN 2005, Montreal, Canada (October 2005)
11. Ravelomanana, V.: Extremal properties of three-dimensional sensor networks with applications. IEEE Transactions on Mobile Computing 3(3), 246–257 (2004)
12. Wan, P.-J., Yi, C.-W., Yao, F., Jia, X.: Asymptotic critical transmission radius for greedy forward routing in wireless ad hoc networks. In: Proc. of ACM Mobihoc (2006)
13. Wang, Y., Li, F., Dahlberg, T.: Power efficient 3-dimensional topology control for ad hoc and sensor networks. In: Proc. of IEEE GlobeCom (2006)
14. Xie, P., Cui, J.-H., Lao, L.: VBF: Vector-based forwarding protocol for underwater sensor networks. In: Proceedings of IFIP Networking 2006 (2006)